Eur. Phys. J. A **24**, 373–378 (2005)
DOI 10.1140/epja/i2004-10237-y

THE EUROPEAN PHYSICAL JOURNAL A

# Angular momenta of fission fragments in the $\alpha$-accompanied fission of $^{252}$Cf

M. Jandel[1,4,a], J. Kliman[1,4], L. Krupa[1,4], M. Morháč[1,4], J.H. Hamilton[2], J. Kormicki[2], A.V. Ramayya[2], J.K. Hwang[2], Y.X. Luo[2], D. Fong[2], P. Gore[2], G.M. Ter-Akopian[4], Yu.Ts. Oganessian[4], A.M. Rodin[4], A.S. Fomichev[4], G.S. Popeko[4], A.V. Daniel[4], J.O. Rasmussen[5], A.O. Macchiavelli[5], M.A. Stoyer[6], R. Donangelo[7], and J.D. Cole[8]

[1] Department of Nuclear Physics, Slovak Academy of Sciences, Dubravska cesta 9, Bratislava, Slovak Republic
[2] Department of Physics, Vanderbilt University, Nashville, TN 37235, USA
[3] Joint Institute for Heavy Ion Research, Oak Ridge, TN 37835, USA
[4] Flerov Laboratory for Nuclear Reactions, Joint Institute for Nuclear Research, Dubna, Russia
[5] Lawrence Berkeley National Laboratory, Berkeley, CA 94720, USA
[6] Lawrence Livermore National Laboratory, Livermore, CA 94550, USA
[7] Instituto de Física, Universidade Federal do Rio de Janeiro, 21945-970 Rio de Janeiro, Brazil
[8] Idaho National Engineering and Environmental Laboratory, Idaho Falls, ID 83415, USA

Received: 15 January 2005 / Revised version: 10 April 2005 /
Published online: 27 May 2005 – 
Communicated by C. Signorini

**Abstract.** For the first time, average angular momenta of the ternary fission fragments $^{100,102}$Zr,$^{106}$Mo, $^{144,146}$Ba and $^{138,140,142}$Xe from the $\alpha$-accompanied fission of $^{252}$Cf were obtained from relative intensities of prompt $\gamma$-ray transitions with the use of the statistical model calculation. Average values of the angular momenta were compared with the corresponding values for the same fission fragments from the binary fission of $^{252}$Cf. Results indicate the presence of a decreasing trend in the average values of angular momenta induced in ternary fission fragments compared to the same binary fission fragments. On the average, the total angular momentum extracted for ternary fission fragments is $\sim$1.4 $\hbar$ lower than in binary fission. Consequently, results indicate that the mechanism of the ternary $\alpha$-particles emission may directly effect an induction of angular momenta of fission fragments, and possible scenarios of such mechanisms are discussed. Further, the dependence of the angular momenta of $^{106}$Mo and $^{140}$Xe on the number of emitted neutrons from correlated pairs of primary fragments was obtained also showing a decreasing dependence of average angular momenta with increasing number of emitted neutrons. Consequences are briefly discussed.

**PACS.** 25.85.Ca Spontaneous fission – 29.30.Kv X- and gamma-ray spectroscopy

## 1 Introduction

Angular-momentum distribution of fission fragments in the spontaneous fission arises from the statistical population of collective modes [1]. A ground-state population of bending oscillations at the scission point inducing a finite distribution of the rotational angular momentum was introduced in [2]. The close relation between the fragment angular momentum and the dynamics of the fissioning nucleus at its final stages is the reason of the great interest in studies of the angular-momentum distribution of fission fragments in theory [3–5] and experiment [6–11]. Common procedures for the determination of the angular-momentum distribution in the nucleus are based on the statistical model analysis which was developed in [12] to explain isomeric yield ratios in neutron capture and charged-particle–induced reactions. Similarly, it can be applied to the fission process assuming a defined initial distribution of angular momentum in the primary fission fragment at the scission point. After the statistical decay of primary fission fragments through the emission of prompt $\gamma$-rays and neutrons, the de-excitation in the well-known rotational bands occurs via the $\gamma$-ray emission to the ground state of secondary fission fragments. The last stage of the de-excitation is thoroughly mapped by fission fragment spectroscopy experiments and the energy levels with assigned spin are widely tabulated [13]. From the relative intensities of the known transitions with assigned spin, one may deduce primary fragments' angular momenta. Angular momenta of individual fission fragments from the spontaneous fission of $^{252}$Cf were obtained using relative intensities of the prompt $\gamma$-ray transitions for the first time in [7]. The same approach was used in [8]

[a] e-mail: jandel@comp.tamu.edu

in order to extract the dependence of average angular momenta on the number of emitted neutrons from the correlated pairs. A similar analysis is done in this work, where, for the first time, the angular momenta of fragments from the $\alpha$-accompanied ternary fission of $^{252}$Cf are extracted.

## 2 Experiment and data analysis

The details of experiment in which prompt $\gamma$-rays from fission fragments of $^{252}$Cf were measured in coincidence with ternary particles are given in [14] and will be only briefly discussed here. The intensity of the $^{252}$Cf source was $3 \times 10^4$ spontaneous fission events per second. An active layer with a diameter of 3 mm was deposited on a 1.5 $\mu$m Ti foil and covered from both sides with gold foils in order to stop the fission fragments and minimize the Doppler broadening in prompt $\gamma$-ray spectra. Light charged particles (LCP) were detected by eight $\Delta E$-$E$ silicon telescopes. They provided full absorption of LCP particles and unique identification of $\alpha$, Be and C particles. Telescopes provided the trigger signal for Gammasphere measuring prompt $\gamma$-rays from fission fragments. During the three-week-long experiment $5.9 \times 10^6$ of $\alpha$-ternary fission events were collected and corresponding $\sim 13.5 \times 10^6$ prompt $\gamma$-rays were measured in coincidence with $\alpha$-ternary particles. The statistical model analysis [7,12] was used for the determination of the fragments' average angular momenta. The analysis consisted in four steps: i) determination of relative intensities of $\gamma$-ray transitions in the ground-state band from measured prompt $\gamma$-ray spectra, ii) determination of the contribution of primary fragments to the yield of given secondary fragments iii) calculation of the statistical decay through $\gamma$-ray and neutron emission from primary fragments with a given initial angular momentum, iv) obtaining the dependence of ratios of transition intensities in the ground-state band, *i.e.* $I(6^+ \rightarrow 4^+)/I(4^+ \rightarrow 2^+)$, $I(8^+ \rightarrow 6^+)/I(4^+ \rightarrow 2^+)$ etc., on the primary angular-momentum distribution from the statistical analysis. Only even-mass fragments were involved in the analysis and only $E2$ quadrupole transitions in the ground-state band were analyzed with the assumption that the ground-state band is directly fed after the statistical emission. The values of initial angular momenta of fission fragments were then deduced by comparing the calculated values of transition yield ratios from step iv) with the experimental ratios from step i). Consecutive steps of the extraction of average angular momenta released in the ternary fission process are described in more detail in the following text.

The identification of fission fragments was performed using fission fragment spectroscopy methods [8,15,16]. By gating in the $\gamma$-$\gamma$ coincidence matrix on lowest-lying transitions $2^+ \rightarrow 0^+$ in the ground-state band of an even-mass fission fragment, the peaks of higher transitions in the rotational $E2$ band appear in the gated $\gamma$-ray spectra. In fig. 1, a coincidence spectrum obtained by gating on the $2^+ \rightarrow 0^+$ transition in $^{100}$Zr with an energy of 212 keV is shown for illustration. In the same manner, the $\gamma$-ray transitions in sister fragments from correlated pairs can also be identified with a unique determination of the number of

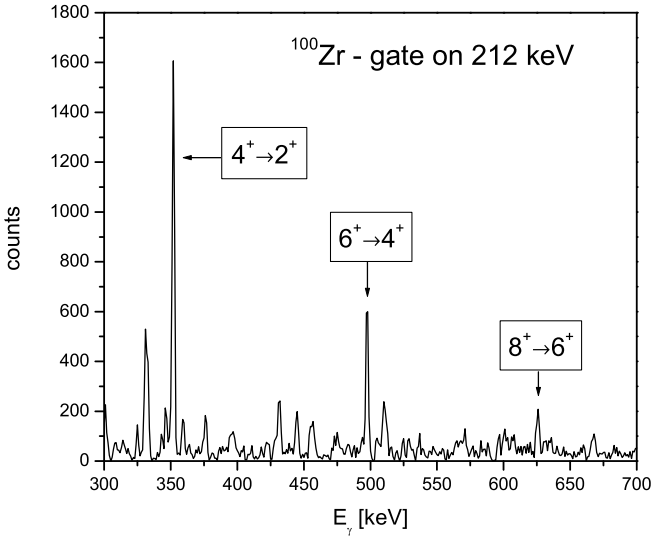


**Fig. 1.** Coincidence $\gamma$-ray spectrum obtained by gating on the $2^+ \rightarrow 0^+$ transition in $^{100}$Zr with an energy of 212 keV.

emitted neutrons. In case of an individual fragments analysis, the lowest transition appears to be $4^+ \rightarrow 2^+$, and the ratios of transition intensities were determined relative to this transition. The ratios were obtained for eight ternary fission fragments: $^{100,102}$Zr, $^{144,146}$Ba, $^{106}$Mo and $^{138,140,142}$Xe. They are shown in table 1. The inaccuracy of the obtained values of transition intensities ratios is up to 5% but not higher. It should be mentioned that the background in prompt $\gamma$-ray spectra was efficiently eliminated. The background subtraction was performed already in the $\gamma$-$\gamma$ matrix of coincidences using a two-dimensional subtraction based on the algorithm presented in [17]. This is the correct way to deal with the background elimination rather than using one-dimensional methods of background subtraction from spectra obtained from the matrix of $\gamma$-$\gamma$ coincidences by gating. The main reason for this is that the background under the peak of interest may have different amplitudes in both directions of the matrix of $\gamma$-$\gamma$ coincidences. The fitting of peaks of interest was done by procedures requiring that the full width of peaks at half-maximum is equal to that obtained from the calibration of Gammasphere.

The matrix of $\gamma$-$\gamma$ coincidences provided the information on yields of correlated secondary fragment pairs, *i.e.*, the pairs of fragments as they appear after the emission of prompt neutrons and $\gamma$-rays. In order to determine the contribution of primary fragments to the yield of given secondary fragments, mass and excitation energy distribution of primary fragments was extracted from experimental yields of correlated ternary fission fragment pairs by the unfolding procedure. The method was reported by the present authors elsewhere [18] and is briefly summarized in the appendix. The procedure was based on the fit of secondary fragments yields obtained from experiment and by calculation [8]. The primary fragments' mass distribution was obtained for two $\alpha$-ternary charge splits Zr-$\alpha$-Ba and Mo-$\alpha$-Xe with mean primary masses 102.7/145.3 and

**Table 1.** Intensities of higher transitions $I_{64}$ and $I_{108}$ relative to the $I_{42}$ transition. $I_{42}$, $I_{64}$ and $I_{108}$ represent intensities of the $4^+ \to 2^+$, $6^+ \to 4^+$ and $10^+ \to 8^+$ transitions, respectively, and $\langle n \rangle$ is the mean number of emitted neutrons.

| Ratio | $^{100}$Zr | $^{102}$Zr | $^{106}$Mo | $^{144}$Ba | $^{146}$Ba | $^{138}$Xe | $^{140}$Xe | $^{142}$Xe |
|---|---|---|---|---|---|---|---|---|
| $I_{64}/I_{42}$ | 0.47 | 0.46 | 0.48 | 0.69 | 0.45 | 0.51 | 0.57 | 0.56 |
| $I_{86}/I_{42}$ | 0.19 | 0.26 | 0.09 | 0.30 | 0.27 | 0.26 | 0.29 | 0.30 |
| $I_{108}/I_{42}$ | | | | | | 0.11 | 0.12 | |
| $\langle n \rangle$ | 1.43 | 1.01 | 1.58 | 1.03 | 0.56 | 2.49 | 1.63 | 1.28 |

**Table 2.** The contribution of primary fragments to the yield of a given secondary fragment. $n$ corresponds to the number of emitted neutrons from primary fragments. In the first row, analyzed secondary fragments are shown.

| $n$ | $^{100}$Zr | $^{102}$Zr | $^{144}$Ba | $^{146}$Ba | $^{106}$Mo | $^{138}$Xe | $^{140}$Xe | $^{142}$Xe |
|---|---|---|---|---|---|---|---|---|
| 0 | 0.32 | 0.35 | 0.06 | 0.14 | 0.68 | 0.00 | 0.03 | 0.06 |
| 1 | 0.20 | 0.30 | 0.48 | 0.70 | 0.19 | 0.26 | 0.54 | 0.66 |
| 2 | 0.21 | 0.35 | 0.36 | 0.16 | 0.04 | 0.34 | 0.30 | 0.23 |
| 3 | 0.27 | | 0.02 | | 0.10 | 0.03 | 0.03 | 0.06 |
| 4 | | | 0.09 | | | 0.36 | 0.10 | |

**Table 3.** Average angular momenta for ternary fission fragments $\langle J \rangle_{\rm tf}$ (this work) and binary fission fragments $\langle J \rangle_{\rm bf}$ in $^{252}$Cf (s.f.) [7].

| | Light fragments | | | Heavy Fragments | | | | |
|---|---|---|---|---|---|---|---|---|
| | $^{100}$Zr | $^{102}$Zr | $^{106}$Mo | $^{144}$Ba | $^{146}$Ba | $^{138}$Xe | $^{140}$Xe | $^{142}$Xe |
| $\langle J \rangle_{\rm tf}$ | 4.3(3) | 4.5(3) | 4.15(25) | 6.3(3) | 4.6(3) | 5.3(3) | 5.6(3) | 5.3(3) |
| $\langle J \rangle_{\rm bf}$ | 5.0 | 5.35 | 4.63 | 5.87 | 4.72 | 5.46 | 8.35 | |

106.3/141.7, respectively. Here we only present the results of the unfolding procedure concerning relative contributions of individual primary fragments to the yield of a given secondary fragment. They are summarized in table 2.

The form of the initial angular-momentum distribution of primary fission fragments is given by [7]

$$P(J) \propto (2J+1)e^{-J(J+1)/B^2}, \qquad (1)$$

where $P(J)$ is the probability distribution for each value $J$ of angular momentum and $B$ is the angular-momentum parameter approximately equal to the r.m.s. value of $(J + 0.5)$. The average angular momentum $\langle J \rangle$ is then defined by

$$\langle J \rangle = \frac{\sum_i P(J_i)J_i}{\sum_i P(J_i)} = B\frac{\sqrt{\pi}}{2} - \frac{1}{2}. \qquad (2)$$

The process of de-excitation of the fission fragments was simulated using a code PACE2 [19] which follows the correct procedure for angular coupling at each stage of de-excitation in the framework of Hauser-Feshbach formalism. The calculation was performed for the values of the angular-momentum parameter $B$ varied in the interval 1.5–10 $\hbar$ to obtain a continuous dependence of transition intensity ratios. The nuclear levels of the ground-state band was introduced in the statistical calculation and a direct feeding to the ground-state band after the emission of prompt neutrons and statistical $\gamma$-rays was assumed. Several primary fragments contribute to the final transition intensity ratios in the ground-state band of the individual secondary fragment. The calculation was performed with all primary fragments that contribute to the yield of the analyzed secondary fragment. Excitation energies of primary fragments were calculated from the excitation energy distribution obtained by the unfolding procedure, as a mean weighted value of the excitation energy in the interval where $n$ neutrons are emitted from the primary fragment. The average angular momenta for given secondary fragments were determined by taking the weighted average of the contributions from individual primary fragments (table 2). We used the approximation that each primary fragment would feed the ground-state band of the analyzed secondary fragment equally. To analyze the unequal feeding, the complete transition intensities in all secondary fragments would be needed. However, it is a good approximation when average angular momenta of the primary fragments are deduced.

## 3 Results and discussion

Average values of the angular momentum $\langle J \rangle_{\rm tf}$ are given in table 3, together with the values of the average angular momenta $\langle J \rangle_{\rm bf}$ for the same secondary fragments from the binary fission [7]. A systematic decrease in the average angular momenta $\langle J \rangle_{\rm tf}$ is observed in the results from the ternary fission compared to the $\langle J \rangle_{\rm bf}$ of the fragments in the binary process. The analyzed fragments were divided into the groups of light and heavy fragments in order to estimate the observed decrease from the point of view of the fission process. As is shown in table 3, the value $\langle J \rangle_{\rm tf}$

of light fragments is lower by 0.7(3) $\hbar$ on average compared to the same light-fragment group from binary fission. The heavier fragments from ternary fission release also less angular momentum on the average by 0.7(3) $\hbar$. However, we see a large distribution of $\Delta = \langle J \rangle_{\rm bf} - \langle J \rangle_{\rm tf}$ for the group of heavy fragments with a large standard deviation of 1.2 $\hbar$. This does not allow us to make a definite statement that also the heavy-fragments angular momenta are affected by the emission of a ternary particle. However, we will further use for the discussion the average value of 0.7(3) $\hbar$ also for the heavy fragments. Then, a total difference in the average evaporated angular momentum in binary and ternary process is $\sim 1.4$ $\hbar$.

There are several possible scenarios for an effect of the decrease of $\langle J \rangle$. If one assumes the simple quantal model of initial spin distribution at scission [3] provided that the neck snaps suddenly (in case of ternary fission we would assume sudden double-neck rupture), the width of the angular wave pocket of a fragment will be roughly the angle subtended by the neck before rupture. The r.m.s. average spin at scission would be then reciprocal of the width of the angular wave pocket. The thicker is the neck before rupture, the less angular momentum will be induced on average. In ternary fission one may assume that before the neck's double snapping takes place, there is a light charged particle situated in between fragments. If an $\alpha$-particle is involved, the neck before rupture may be assumed to have a radius around 1.6 fm, which is on average thicker than in binary fission with the corresponding fission fragments, therefore the initial angular momentum will be less in ternary fission than it is in binary.

Another scenario may stem from the following. The angular momentum of fission fragments is induced by collective oscillations at the scission point and a non-negligible contribution to the induced angular momentum is Coulomb excitation [2,3]. Due to the emission of a LCP particle, the distance between centers of mass of both fragments and also between the tips is larger than in binary fission. One may assume that the Coulomb excitation that enhances the angular momenta of fragments would not be so strong in the ternary fission as it is in the binary fission, because the strongest torque is acquired by fragments at small tip distances. This would also result in the decrease of the initial average angular momentum induced on ternary fission fragments. Obviously, an effect of the decrease of the average angular momenta may be the combination of both the scenarios mentioned above.

Finally, we would like to make an important comment based on the preliminary observation of energy levels feeding in fragments from spontaneous fission of $^{252}$Cf. The observed decrease in the average angular momenta of ternary fission fragments in comparison with the ones from binary fission is dependent on the statistical model analysis. However, one may directly observe a decreased feeding of higher-spin states in the ground-state band for all of the analyzed ternary fission fragments compared to the same feedings from binary fission [20]. This indicates that the primary average angular momentum of ternary fission fragments should be lower. In this context, the revision of the data on the angular momentum of binary fission fragments would help in the further discussion concerning the angular-momentum induction and the role of the ternary particle in it. The full analysis of binary fission data to extract the angular momenta is of great interest and will be our aim in the near future, to have the possibility of direct comparison between the ternary and binary fission fragments angular momenta.

**Table 4.** Measured ratios of transition intensities and average angular momenta of fission fragments $^{106}$Mo and $^{140}$Xe in the correlated pairs. The transition intensities were analyzed in the fragment given in the first column, using $\gamma$-ray spectra obtained by gating in the matrix of $\gamma$-$\gamma$ coincidences on the lowest ground-state-band transition in fragments shown in the second column.

| | | $n$ | $I_{42}/I_{20}$ | $I_{64}/I_{20}$ | $\langle J \rangle$ |
|---|---|---|---|---|---|
| $^{106}$Mo | $^{140}$Xe | 2 | 0.65 | - | 4.8(3) |
| $^{106}$Mo | $^{139}$Xe | 3 | 0.53 | - | 3.7(3) |
| $^{106}$Mo | $^{138}$Xe | 4 | 0.49 | - | 3.5(3) |
| $^{140}$Xe | $^{106}$Mo | 2 | 0.80 | 0.50 | 5.8(2) |
| $^{140}$Xe | $^{105}$Mo | 3 | 0.66 | 0.38 | 5.2(3) |
| $^{140}$Xe | $^{104}$Mo | 4 | 0.65 | 0.40 | 5.2(3) |

It was shown in [8] that one can extract the relative ratios of transition intensities for fragments in correlated pairs, so that the dependence of the mean angular momenta of fission fragments on the number of emitted neutrons can be obtained. In this manner we obtained the ratios of transition intensities in $^{106}$Mo relative to the $2^+ \rightarrow 0^+$ transition from the spectra obtained by gating on the transitions leading to the ground state of $^{138,139,140}$Xe (2–4 neutrons emitted). Similarly, this was achieved for $^{140}$Xe, when gating in the $\gamma$-$\gamma$ matrix of coincidences on lowest transitions leading to the ground state in $^{104}$Mo, $^{105}$Mo and $^{106}$Mo. In table 4 the obtained ratios of transition intensities relative to the lowest transition intensity are given together with the number of emitted neutrons for each correlated pair. The average angular momenta of $^{106}$Mo and $^{140}$Xe are given in the last column of table 4. The behavior of the mean angular momenta as a function of number of emitted neutrons from the correlated pairs of fission fragments (see fig. 2) is in close analogy to the results from binary fission [8], where the mean angular momentum decreases with increasing number of evaporated neutrons. The decrease of the angular momentum with increasing number of neutrons is a direct consequence of the fact that each neutron takes approximately 0.6 $\hbar$ of angular momentum away from the fragment. Fission fragments are in this case closer to their ground state or, in other words, the entry line is closer to the yrast line [21]. This is also in an agreement with the assumption of equilibrium between collective degrees of freedom at scission [1,2,8].

It is obvious that to reveal all the physical content and the details lying behind the induced angular momenta in binary and ternary fission fragments, more experiments have to be carried out and more fission fragments have to be analyzed. In this context, a study of cold-fission modes is of a great interest, because here we expect a

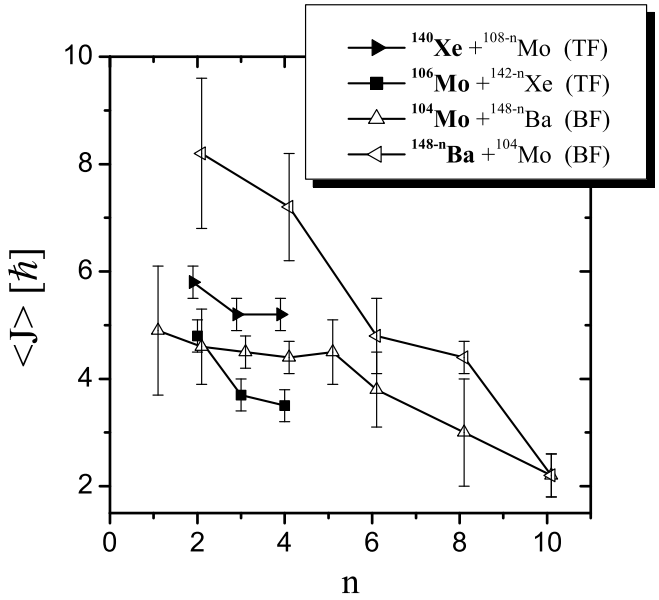


**Fig. 2.** Mean angular momenta of $\alpha$-accompanied fission fragments (TF) $^{106}$Mo,$^{140}$Xe and binary fission fragments (BF) $^{104}$Mo,$^{148-n}$Ba in correlated pairs as a function of the number $n$ of emitted neutrons. Mean angular momenta of binary fission fragments are taken from [8].

maximum in the induced angular momentum on fission fragment and comparison between BF and TF can bring a clear picture as the neutron emission from the fragments is absent. In such case, the feeding of ground-state-band energy levels is direct and there is no need for statistical calculation which smears results significantly. We believe that the presented results will encourage the theoretical work over the formation of the fragment spins and also the dynamics of the fission process itself as the ternary particle can be considered as a reminiscence of the neck of the fissionning nucleus and, as shown in this work, its effect on the induced angular momenta is not negligible.

The work was partially supported by the Grant Agency of Slovak republic through contract GAV 2/1132/21. Research at Vanderbilt University is supported in part by the U.S. Department of Energy under grant No. DE-FG05-88ER40407. Work at Idaho National Engineering Laboratory is supported by the U.S. Department of Energy under contract No. DE-AC07-76ID01570. The work at LLNL was performed under the auspices of the U.S. Department of Energy under contract No. W-7405-ENG-48, and that of LBNL under contract No. DE-AC03-76SF00098. The Joint Institute for Heavy Ion Research is supported by the member institutes, the University of Tennessee, Vanderbilt University and the U.S. Department of Energy. Authors would like to thank F. Goennenwein for comments and fruitful discussions.

## Appendix A.

The unfolding procedure was used for the extraction the characteristics of primary fragments distribution similar to the one used in [8], where experimental information on correlated secondary fragment yields in binary fission was used for the determination of primary fragments' mass and excitation energy distribution. Yields of primary fragments $Y(A_L, A_H|Z_L, Z_H)$ can be connected to the yields of secondary fragments by

$$Y^{\mathrm{calc}}(A'_L, A'_H|Z_L, Z_H) = \sum_{(A_L,A_H)} Y(A_L, A_H|Z_L, Z_H) \times I_L \times I_H, \tag{A.1}$$

$$I_L = \int F(E^*_L, A_L)\, P_n(E^*_L, A_L)\, \delta(A_L - A'_L - n)\, \mathrm{d}E,$$
$$I_H = \int F(E^*_H, A_H)\, P_n(E^*_H, A_H)\, \delta(A_H - A'_H - n)\, \mathrm{d}E, \tag{A.2}$$

where $F(E^*, A)$ is the excitation energy distribution of each primary fission fragment, $P_n(E^*_H, A_H)$ is the probability of evaporation of $n$ neutrons from a primary fragment ($n = A - A'$). Primary fragments characteristics are obtained minimizing

$$\chi^2 = \frac{1}{N_{\mathrm{exp}} - N_{\mathrm{par}}} \times \sum \left[ \frac{Y^{\mathrm{exp}}(A'_L, A'_H|Z_L, Z_H) - Y^{\mathrm{calc}}(A'_L, A'_H|Z_L, Z_H)}{\sigma_{\mathrm{exp}}(A'_L, A'_H|Z_L, Z_H)} \right]^2. \tag{A.3}$$

The following assumptions were made to reduce the number of free parameter of the procedure. We assumed that the excitation energy distribution as well as the primary fragment mass distribution are Gaussian. Mean excitation energies of heavy and light fragments $\langle E^*_{L,H} \rangle$ and their variances $\sigma^2_{L,H}$ obey the following conditions:

$$Q_{\mathrm{fiss}} = \langle TKE \rangle + \langle E^*_L \rangle + \langle E^*_H \rangle, \tag{A.4}$$

$$\sigma^2_{TKE} = \sigma^2_{E^*_L} + \sigma^2_{E^*_H}, \tag{A.5}$$

$$\frac{\sigma^2_{E^*_L}}{\langle E^*_L \rangle} = \frac{\sigma^2_{E^*_H}}{\langle E^*_H \rangle}. \tag{A.6}$$

Mean total kinetic energy $\langle TKE \rangle$ and its variance $\sigma^2_{TKE}$ were assumed to be fixed for a given charge split. As a result of the minimization procedure, yields of correlated primary fragment pairs $Y(A_L, A_H|Z_L, Z_H)$ and the excitation energy distributions $F(E^*_{L,H}, A_{L,H})$ of heavy and light primary fragments were obtained. One is then able to construct the mass distribution of primary fragments and neutron multiplicity distributions for a given charge split from these results.

## References

1. J.R. Nix, W.J. Swiatecki, Nucl. Phys. **71**, 1 (1965).
2. J.O. Rasmussen, W. Norenberg, H.J. Mang, Nucl. Phys. A **136**, 465 (1969).
3. J.O. Rasmussen *et al.*, *Proceedings of the International Conference DANF96, Častá Papiernička, Slovakia, 1996*, edited by J. Kliman, B.I. Pustylnik (JINR, Dubna, 1996) p. 289.
4. S. Misicu, A. Sandulescu, G.M. Ter-Akopian, W. Greiner, Phys. Rev. C **60**, 034613 (1999).

5. T.M. Shneidman, G.G. Adamian, N.V. Antonenko, S.P. Ivanova, R.V. Jolos, W. Scheid, Phys. Rev. C **65**, 064302 (2002)
6. D.G. Sarantites, G.E. Gordon, C.D. Coryyell, Phys. Rev. **138**, B353 (1965).
7. J.B. Wilhelmy *et al.*, Phys. Rev. C **5**, 2041 (1972).
8. G.M. Ter-Akopian *et al.*, Phys. Rev. C **55**, 1146 (1997).
9. I.N. Vishnevski *et al.*, Jad. Fiz. **61**, 1562 (1998).
10. Yu.N. Kopach *et al.*, Phys. Rev. Lett. **82**, 303 (1999).
11. H. Naik, S.P. Dange, R.J. Singh, Eur. Phys. J. A **7**, 377 (2000).
12. J.R. Huizenga, R. Vandenbosch, Phys. Rev. **120**, 1305 (1960).
13. `http://ie.lbl.gov/isoexpl/isoexpl.htm`.
14. M. Jandel *et al.*, J. Phys. G **28**, 2893 (2002).
15. E. Cheifetz, J.B. Wilhelmy, R.C. Jared, S.G. Thompson, Phys. Rev. C **4**, 1913 (1971).
16. R. Aryaeinejad *et al.*, Phys. Rev. C **48**, 566 (1993).
17. M. Morhac *et al.*, Nucl. Instrum. Methods A **401**, 113 (1997).
18. M. Jandel *et al.*, *Proceeding of the International Conference on Fission and Properties of Neutron-Rich Nuclei, Sanibel Island, Florida, 2002*, edited by. J.H. Hamilton, A.V. Ramayya, H.K. Carter (World Scientific, Singapore, 2003) p. 448.
19. A. Gavron, Phys. Rev. C **21**, 230 (1980).
20. *Level schemes of fragments from spontaneous fission of* $^{252}$Cf, Vanderbilt University, unpublished.
21. D.L. Hillis *et al.*, Nucl. Phys. A **325**, 216 (1979).